FEBS Letters 584 (2010) 2539–2547

FEBS Letters

journal homepage: www.FEBSLetters.org

Review

Tricks of the trade used to accelerate high-resolution structure determination of membrane proteins

Yo Sonoda [a,1], Alex Cameron [e], Simon Newstead [a,2], Hiroshi Omote [c], Yoshinori Moriyama [c], Michihiro Kasahara [b], So Iwata [a,d,e,*], David Drew [a,**]

[a] Division of Molecular Biosciences, Imperial College London, London SW7 2AZ, UK
[b] Laboratory of Biophysics, School of Medicine, Teikyo University, Hachioji, Tokyo 192-0395, Japan
[c] Laboratory of Membrane Biochemistry, Okayama University Graduate School of Medicine, Dentistry and Pharmaceutical Sciences, Okayama 700-8530, Japan
[d] Japan Science and Technology Agency, ERATO, Human Crystallography Project, Yoshida Konoe, Sakyo-ku, Kyoto 606-851, Japan
[e] Membrane Protein Laboratory, Diamond Light Source, Harwell Science and Innovation Campus, Didcot, Chilton, Oxfordshire OX11 0QX, UK

ARTICLE INFO

Article history:
Received 7 March 2010
Revised 1 April 2010
Accepted 8 April 2010
Available online 13 April 2010

Edited by Jan Rydström

Keywords:
Membrane protein
X-ray structure
Fluorescence-detection size-exclusion chromatography
Green Fluorescent Protein
Mammalian transporter

ABSTRACT

The rate at which X-ray structures of membrane proteins are solved is on a par with that of soluble proteins in the late 1970s. There are still many obstacles facing the membrane protein structural community. Recently, there have been several technical achievements in the field that have started to dramatically accelerate structural studies. Here, we summarize these so-called 'tricks-of-the-trade' and include case studies of several mammalian transporters.

1. Introduction

Until the first membrane protein crystal structure was solved in 1985 [1], structural analysis of membrane proteins by X-ray crystallography was thought to be an unrealizable challenge. Since then, through the tremendous painstaking effort of many research groups more than 200 unique membrane protein structures have been solved. As more than 40% of small molecule drug targets are aimed at membrane proteins, each high-resolution structure is eagerly anticipated by both academia and the pharmaceutical industry [2]. The challenges, however, still remain the same. Chiefly, how to produce enough functional material and how to coax the formation of crystals in the presence of detergent that inherently restricts protein contacts? Here we will discuss some technical advances in the field. They are based on the premise that obtaining structures of membrane proteins is hard to rationalize from conception. These advances do not make the challenges go away, but instead, aim to make the process quicker by recognizing which parameters are the most important to optimize.

2. Fluorescence-based membrane protein overexpression and monodispersity screening

What is the best parameter to screen for first? If we work backwards and analyze samples of membrane proteins that form crystals, we find that in the majority of cases the membrane proteins that form crystals tend to migrate as a single uniform peak on a

Abbreviations: SEC, size-exclusion chromatography; DDM, *n*-dodecyl-β-D-maltopyranoside; GFP, Green Fluorescent Protein; FSEC, fluorescence-detection size-exclusion chromatography; OG, *n*-octyl-β-D-maltopyranoside; OTG, *n*-octyl-β-D-thiomaltopyranoside; NM, *n*-nonyl-β-D-maltopyranoside; CPM, N-[4-(7-diethylamino-4-methyl-3-coumarinyl)phenyl]maleimide; TM, transmembrane; DM, *n*-decyl-β-D-maltopyranoside; CHS, cholesteryl hemisuccinate; TEV, tobacco etch virus protease; IMAC, immobilized metal affinity chromatography; Ni-NTA, nickel-nitrilotriacetic acid; $C_{12}E_8$, dodecyl octaethylene glycol ether; $C_{12}E_9$, dodecyl nonaethylene glycol ether; LDAO, *n*-dodecyl-N,N-dimethylamine-*n*-oxide; NG, *n*-nonyl-β-D-glucoside

* Corresponding author at: Division of Molecular Biosciences, Imperial College London, London SW7 2AZ, UK.
** Corresponding author.
E-mail addresses: s.iwata@imperial.ac.uk (S. Iwata), d.drew@imperial.ac.uk (D. Drew).
[1] Present address: Drug Discovery Research Department, Central Research Laboratories, Kaken Pharmaceutical Co. Ltd, 14 Shinomiya-minamigawara, Yamashina, Kyoto 607-8042, Japan.
[2] Present address: Department of Biochemistry, University of Oxford, South Parks Road, Oxford OX1 3QU, UK.

0014-5793/$36.00 © 2010 Published by Elsevier B.V. on behalf of the Federation of European Biochemical Societies.
doi:10.1016/j.febslet.2010.04.015

size-exclusion column. The degree of symmetry and broadness of the peak after size-exclusion chromatography (SEC) is an indication of the "monodispersity" of the protein solution, or more precisely the protein detergent complex. In fact, the choice of detergent that is used to keep the protein in solution is one of the most important parameters in dealing with membrane proteins. How do we choose this detergent? A good starting point is to first purify the membrane protein in a detergent, such as *n*-dodecyl-β-D-maltopyranoside (DDM) that has a long alkyl chain, and consequently is relatively mild, but as we will later discuss is not always the best for crystallization. The sample is then injected onto a size-exclusion column equilibrated in several different detergents usually of a smaller micelle-size to find other suitable matches. That seems reasonable if you can purify milligram amounts of functional material, but what if you do not know whether you are able to overexpress, let alone purify the membrane protein in the first place?

Our method of choice is to couple the overexpression of all our membrane proteins with a C-terminal Green Fluorescent Protein (GFP) tag. Although this idea was originally conceived as a folding indicator for soluble proteins [3], it was important to verify the use for membrane proteins as they undergo a very different folding pathway [4]. Arguably it is a more reliable folding indicator for membrane proteins than for globular proteins, as GFP can impose physical restraints on the folding of soluble fusion partners in *Escherichia coli* [5]. In contrast, membrane proteins fold co-translationally, which means that GFP can only fold and become fluorescent once the upstream membrane protein has first integrated into the lipid bilayer [6]. If translation of the membrane protein is uncoupled from the translocon, then synthesis follows into the cytoplasm wherein the membrane protein aggregates to form inclusion bodies. In this scenario the GFP tag does not have the possibility to fold to become fluorescent. The amount of membrane-integrated expression can be calculated by monitoring GFP fluorescence in whole cells spectrophotometrically. Because GFP remains folded in SDS, the integrity of the fusion can also be detected after SDS–PAGE by in-gel fluorescence [7]. The fluorescence is quantifiable, specific, and sensitive down to 5 ng and is faster and more efficient than either Western blotting or Coomassie staining [7]. We use GFP-based pipelines in *E. coli* and *Saccharomyces cerevisiae* as general workhorses for pro- and eukaryotic membrane protein overexpression and purification [7–10]. However, the same approaches can be applied to transient expression in mammalian and insect cells [11]. There are already many excellent reviews on the pros and cons of each expression host and how to optimize membrane protein overexpression and for this reason they are not expanded on here, e.g. [12–14].

The best utility of the GFP-tag is, however, not in overexpression screening but rather in being able to monitor the monodispersity of the sample in detergent-solubilized whole-cells or membranes prior to purification by Fluorescence-detection size-exclusion chromatography (FSEC) [11]. This simple 'trick' was developed in the lab of Eric Gouaux as a pre-crystallization screening tool on the basis that fluorescence detection in crude samples saves considerable time, resources and requires little material. In our laboratory we generally exploit the natural variation of specific proteins among different organisms to find those that are most suitable for crystallization; the GFP method is ideal in this regard [10]. Once a suitable candidate is selected, mutants with improved monodispersity can be screened for as elegantly highlighted by the use of this strategy to obtain the structure of the rat ionotropic glutamate AMPA receptor [15]. The reason FSEC is so useful, especially in the absence of a suitable functional assay, is that we can already monitor at the first-step what we are finally aiming for. It allows some initial judge of the quality of membrane protein produced, since the amount of membrane-integrated expression bears no resemblance to whether the membrane protein has actually obtained the correct fold for function [16]. Indeed, we monitored the overexpression and monodispersity of ~50 different eukaryotic transporters by GFP-based fluorescence using the methodology just described and tailored for the yeast expression host *S. cerevisiae* [17]. After comparing FSEC traces to the level of whole-cell fluorescence we found little correlation [10]. Of the eukaryotic transporters that we could produce to 1 mg per liter or more in *S. cerevisiae* only 60% were monodisperse in DDM [10]. A good illustration of the potential of FSEC in selecting homologues this way is that out of the number of transporter families we have targeted to date we find that ~80% of those monodisperse in DDM can be later purified in this detergent and 40% of this number crystallize (unpublished data). To exploit FSEC fully we compare the broadness of our FSEC traces to set membrane protein standard peaks known to crystallize in the detergent we are screening.

One potential drawback of using GFP, as with any tag, is that it could hinder protein function. Indeed, there are a number of reported examples where a GFP fusion was shown to affect function, see e.g. [18]. However, in the majority of cases GFP is a remarkably benign protein fusion. Imaging the fluorescence acquired from C-terminal GFP-fusions it was possible to designate the organelle localization for 75% of the *S. cerevisiae* proteome, with only a small number of mistargeted proteins; predominantly those that harbor an C-terminal localization signal [19]. The wide use of GFP in localization studies is important, because for many membrane proteins there exists some prior knowledge as to whether a GFP fusion affects function. If a C-terminal GFP fusion does inhibit function, there is the option to construct an N-terminal GFP fusion instead [20]. However, because an N-terminal GFP fusion is more likely to disrupt membrane protein targeting and as GFP can now be translated at a higher rate than the down-stream membrane protein – resulting in non-tagged GFP expression – we prefer to make a C-terminal GFP fusion first. One limitation for expression in *E. coli* is that the C-terminal (or N-terminal) tail of the membrane protein is cytoplasmic, as GFP does not fold efficiently across the bacterial inner membrane via the Sec translocase [21]. However, ~80% of membrane proteins do have a C_{in} topology [22], and for C_{out} topologies, one further option is to consider the addition of an extra helix, e.g. from glycophorin A (GpA). This approach was first successfully applied to the functional expression of the human sodium glucose cotransporter and more recently to a modest number of different transporters [23,24]. In addition to GFP there are many other tag-probe fluorescent labeling methods, because of the limitation of protein fusions it is likely a matter of time before a fluorescent probe supersedes the first-choice use of GFP [25].

3. Detergent selection and stability consideration for obtaining material for diffraction-grade membrane protein crystals

Even if functional milligram amounts of homogenous sample are obtainable, there is another enormous challenge before obtaining a crystal structure of a membrane protein. The detergent that is necessary to keep the protein stable in solution can often prevent essential crystal contacts [26]. For this reason, anecdotally it is more difficult to optimize growth of high order X-ray diffracting crystals in mild detergents, which have longer acyl chains and encompass more of the protein. If we compare the most successful crystallization detergents [17], we find that structures solved in DDM are, on average, of lower resolution compared to those detergents that have been the next most successful (Fig. 1a). Most transporters have been crystallized in DDM [17], and indeed, the median resolution for this family is the poorest at ~3.3 Å

(Fig. 1b). In addition to the fact that many transporters are quite dynamic, which likely precludes their crystallization in a short-chain detergent, a large fraction of deposited structures are of the secondary-active type. These transporters typically lack large hydrophilic domains and perhaps, not surprisingly, we find that no native X-ray structure of a secondary-active transporter has been solved to <2.9–3.0 Å in DDM, but has in either of the short-chain detergents DM (sodium galactose transporter vSGLT, 2.70 Å [27]), NM (benzyl-hydantoin transporter MhpI, 2.85 Å [28]), OG (leucine transporter LeuT, 1.6 Å [29]), or OTG (Na^+-independent amino acid transporter ApcT, 2.35 Å) [30]. Clearly, for proteins such as the secondary-active transporters that do not crystallize in a small chain detergent a 3–4 Å-resolution structure is better than no structure at all. However, there is the caveat that as more structures of similar proteins are becoming available (e.g. the recent structures with the LeuT-fold [29]) the goal is not to see the overall architecture of the protein but rather to be able to decipher the structural details and this requires higher resolution.

There are two complementary strategies used by our laboratory and others to work around this inherent problem. The first approach is to co-crystallize with a monoclonal antibody or some protein fusion, as an extra soluble domain will increase the accessible surface area for crystal contacts. The excellent utility of monoclonal Ab co-crystallization was first proven possible by the crystal structure of cytochrome *c* oxidase complexed with an Fv fragment [31] and since then several membrane protein co-crystal structures predominantly with Fab fragments, e.g. [32,33]. The *E. coli* H^+/Cl^- exchanger highlights a nice example of the higher resolution that can be afforded by this approach; Fab fragment co-crystallized improves structural resolution from 3.5 to 2.5 Å [34,35]. As you might expect good X-ray diffraction may not be obtainable without the Fab fragment. Moreover as more groups aim towards mammalian membrane protein structures, due to an apparent lack of stability in short-chain detergents, it is likely Fab fragment co-crystallization will become increasingly popular. In addition to improving crystallization, Fab fragments have an advantage in that they can be used for phasing. The advantage of phasing this way cannot be underestimated; phasing membrane protein structural data is generally difficult. We anticipate that the use of Fab fragment co-crystallization is likely to be dependent on whether the mammalian membrane proteins used for structural studies do, or do not, contain large hydrophilic domains. For protein fusions, the use of designed ankyrin-repeat proteins (DARPins) in principle offer all the same benefits as Fab fragments [36]. These are made up of variable number of ankyrin units, a naturally occurring 33 residue motif present in many proteins, and specific binders can be screened for using repeat protein libraries by standard screening technologies such as ribosome display. The multidrug efflux-pump AcrB co-crystal DARPin structure was solved to significantly higher resolution at 2.54 Å, and testifies to the potential of this approach [37]. More specific protein fusion strategies has been the remarkable successfulness of the soluble T4–lysozyme fusion to the third intracellular loop of several GPCRs in combination with lipidic-cubic phase crystallization [38] as has recently been well documented, see e.g. [39]. Time will tell whether these insightful approaches can be successfully applied to a greater number of different membrane proteins.

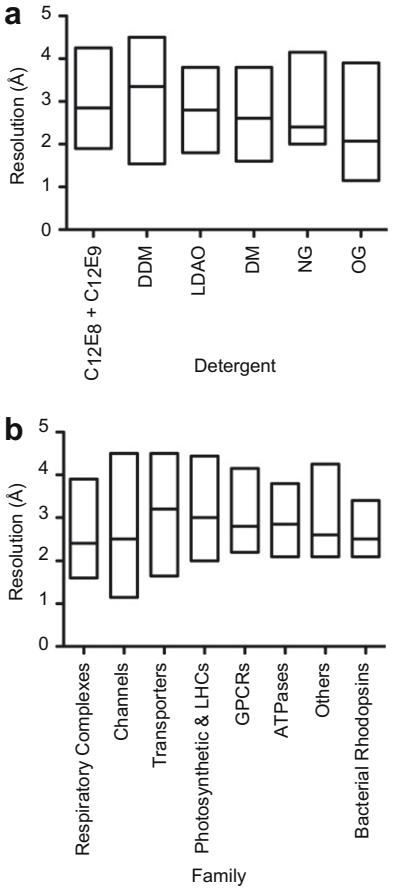

Fig. 1. Exploring the correlation between structural resolution and the type of crystallization detergent. A database was built by collecting the crystallization information from all of the currently available unique alpha-helical MP structures in the PDB. Only structures crystallized using a single defined detergent were included. This task was greatly facilitated by the 'Membrane Proteins of Known 3D Structure' web site from the Stephen White laboratory at UC Irvine (http://blanco.biomol.uci.edu/Membrane_Proteins_xtal.html) (a). Box plots displaying the structural resolution for seven of the most successful crystallization detergents [17]; the middle line in each plot represents the median. (b) Deposited structural resolution for the different membrane protein family members.

Simplistically, the scaffold approach aims to increase crystal contacts in a mild detergent. The alternative strategy is to try and stabilize the membrane protein by mutagenesis so that it now becomes possible to crystallize in a small micelle detergent instead and so exposing a larger surface area of the protein. Encouragingly, as illustrated by Bowie and co-workers membrane proteins, in contrast to soluble proteins, are particularly susceptible to stabilization by mutagenesis, perhaps because there has been less evolutionary pressure applied by the lipid bilayer in comparison to the hydrophobic effect [40,41]. This was the contrasting approach used by Tate and colleagues to obtain the turkey β_1-adrenergic GPCR structure [42]. The conformational thermostabilized receptor was generated by initially screening systematic alanine mutants that bound more of the antagonist dihydroalprenolol than the wild-type receptor after heating [43]. The heterologous expression of the receptor in *E. coli* meant measurements could be made directly from isolated membranes solubilized in DDM. Minor truncations together with six different mutations were finally combined to maximize the stability of the receptor in the antagonist bound-state that when purified from insect cells formed well-ordered crystals in the short-chain detergent OTG [42]. This study is an important conceptual milestone. It adds support to the idea that detergent stability and conformational flexibility are the intrinsically linked factors affecting the growth of well-ordered membrane protein crystals in small micelle-sized detergents.

To monitor the stability of a membrane protein requires some method. In the above case there is a good ligand-binding assay available so that activity could be measured in a relatively straightforward manner, but this is not always the case. In addition to standard biophysical methods such as Circular dichroism spectroscopy [41], one new approach has been to monitor cysteine

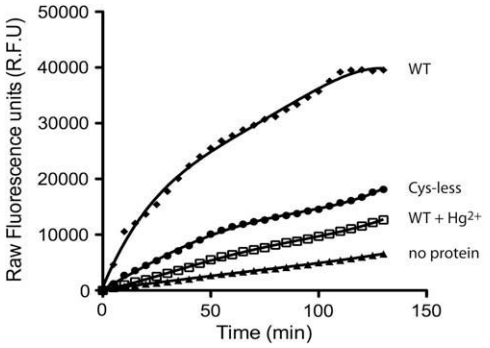

Fig. 2. Using the CPM assay to screen for mercury derivatization. The CPM assay was carried out essentially as described by Stevens and co-workers [44,70]. One microliter of purified bacterial transporter pre-incubated with and without 2.5 mM mercury acetate and subjected to SEC at ~10 mg/ml was added to 150 μl of buffer containing 20 mM Tris–HCl, pH 7.5, 0.1 M NaCl, and detergent at 0.03% DDM in a 96-well black Nunc plate. Three microliters of CPM dye (diluted from a 4 mg/ml stock in dimethyl sulfoxide) at 40 μg/ml was added, clear plate cover set in place, and within 5 min from protein addition fluorescence emission was measured at 463 nm (excitation 387 nm) on the SpectraMax^{2e} plate reader (Molecular Devices) at 40°C. Recordings were measured every 5 min for 130 min with 15 sec shaking between each interval readings; filled diamond, ion transporter with no Hg^{2+} addition; filled circles, Cys-less ion transporter; open squares, ion transporter pre-incubated with Hg^{2+} addition; filled triangles, no protein addition.

accessibility under denaturing conditions using a hydrophobic maleimideprobe N-[4-(7-diethylamino-4-methyl-3-coumarinyl)-phenyl]maleimide (CPM) that becomes fluorescent when it forms a disulfide bond [44]. This assay relies on the premise that most cysteines are buried in transmembranes (TMs) meaning that their accessibility to the dye can be used to evaluate membrane protein stability [44]. Stevens and co-workers developed the proof-of-concept for this assay using three different proteins, and was later applied to the human β_2-adrenergic receptor T4–lysozyme fusion to show that the addition of cholesterol hemisuccinate (CHS) and the partial inverse agonist timolol significantly improves stability [45].

Maleimide fluorescent-conjugated dyes can also be used to help in phasing. When the structure cannot be solved by molecular replacement derivatizing the protein with mercury (Hg^{2+}), which commonly binds to free sulfhydryl groups of cysteine residues, is often one of the most efficient ways to obtain initial phases, see e.g. [46]. If Hg^{2+} is first incubated with the protein and it binds to the –SH groups of cysteine residues then the thiol-based dye is prevented from conjugating [47]. By comparing the loss of in-gel fluorescent band intensity in SDS–PAGE gels with protein that has been incubated with and without Hg^{2+} prior to addition of the dye, it is possible to screen for the optimal Hg^{2+} compound to use and its minimum concentration required for complete derivatization [47]. By using the CPM dye we also find that we can employ a similar strategy to confirm Hg^{2+} derivatization (Fig. 2).

4. Case studies for the optimization of mammalian transporters for structural studies

In Fig. 3, we have outlined a general approach towards obtaining structures of transporters. It should be stressed that although we strive to obtain stable proteins in short-chain detergents this does not mean that we exclude other avenues. More often than not the first crystallization trials performed are carried out with the protein concentrated in DDM. As might be expected we also try to improve any crystals using standard crystallization techniques. In this regard an effective trick is to try different detergents as additives during the crystallization and to screen any crystals obtained for diffraction at the synchrotron. In parallel we continue

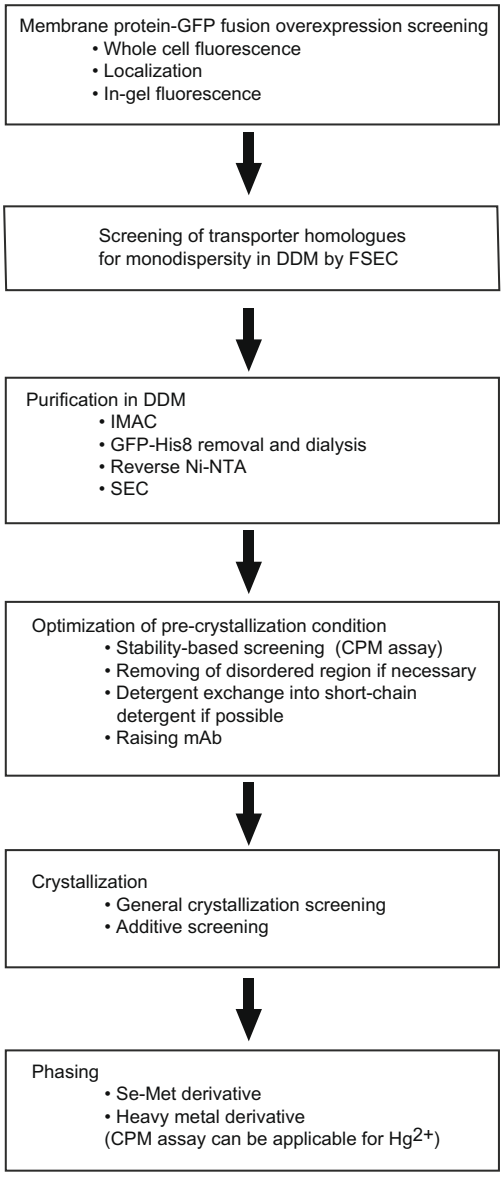

Fig. 3. Schematic flow diagram illustrating the steps towards crystal structures of transporters.

to find other constructs that can be exchanged into short-chain detergents and also consider the antibody approach as this often leads to higher resolution data more quickly than the optimization of a membrane protein crystallized in DDM.

Taken together, although the crystallization screens used by membrane protein structural biologists differ, the general consensus is that success is predominantly based upon having membrane proteins that are monodisperse, functional and stable. Here, we demonstrate the practical application of these methods for isolation of the rat vesicular glutamate transporter VGLUT2 and the human glucose transporter GLUT1.

4.1. Case study 1: vesicular glutamate transporter, VGLUT2

Glutamate is a major excitatory neurotransmitter that plays an essential role for higher neural function such as plasticity, memory, and learning in the central nervous system. Glutamate is stored in synaptic vesicles prior to its depolarization-triggered, calcium-dependent release from neuron terminals [48,49]. VGLUTs are

responsible for the vesicular storage of glutamate and play an essential role in glutamatergic signal transmission in the central nervous system. So far, three isoforms of VGLUT have been identified, VGLUT1, VGLUT2 and VGLUT3 [50]. The helices are highly homologous, ~90% identical in their amino acid sequence, while their N- and C-terminal tails have little homology. VGLUT-mediated L-glutamate transport into synaptic vesicles is dependent on a membrane potential set by the vesicular H^+-ATPase [51]. VGLUT2 is trafficked into vesicular membrane of synaptic cells [48,49], and in COS7 cells distributes into endosomes [52].

Using our standard protocol (see Ref. [9] for step-by-step details) rat VGLUT2–GFP–His_8 overexpresses to nearly 1 mg per liter of *S. cerevisiae* culture as calculated by whole-cell fluorescence [9]. VGLUT2 localizes to the vacuolar membrane in *S. cerevisiae* consistent with the results obtained from mammalian cultures (Fig. 4). Using crude-membranes of VGLUT2 expressing cells for SDS–PAGE, a band at the correct molecular weight was apparent at 80–90 kDa as detected by in-gel fluorescence (Fig. 4b) [7]. 65% of VGLUT2–GFP–His_8 fusion is extracted by Foscholine-12, compared to 58% and 46% for the maltoside detergents DDM and DM, respectively. However, it is clear by FSEC analysis that the major amount of VGLUT2–GFP–His_8 in Foscholine-12 solubilized membranes aggregates (Fig. 4c). VGLUT2–GFP–His_8 is poorly monodisperse in DDM and DM and migrates as a broad profile with a large 'free' GFP peak presumably as a result of degraded VGLUT2 (Fig. 4c). Cholesterol is a stabilizer for several mammalian membrane proteins [53]. As *S. cerevisiae* membranes do not contain cholesterol [54], 0.2% CHS was added to each detergent solubilization test. The addition of CHS improved detergent extraction efficiency and monodispersity of VGLUT2–GFP–His_8 fusion most noticeably in DM-solubilized membranes. Based on FSEC profiles, DM with the addition of CHS was selected as detergents for purification (Fig. 4c).

After identifying suitable purification conditions we could reclone the gene for rat VGLUT2 and purify with a standard hexahistidine tag only [55]. However, our experience is that it is informative to visually monitor purification by fluorescence as it enables each step to be recorded easily, e.g. cell-breakage efficiency, detergent solubilization efficiency, nickel-nitrilotriacetic acid (Ni-NTA) binding efficiency. The C-terminal GFP-fusion encodes an octahistidine-tag with a tobacco etch virus protease (TEV) protease cleavage site for GFP–His_8 removal [6]. After immobilized metal affinity chromatography (IMAC), VGLUT2–GFP–His_8 remained monodisperse,

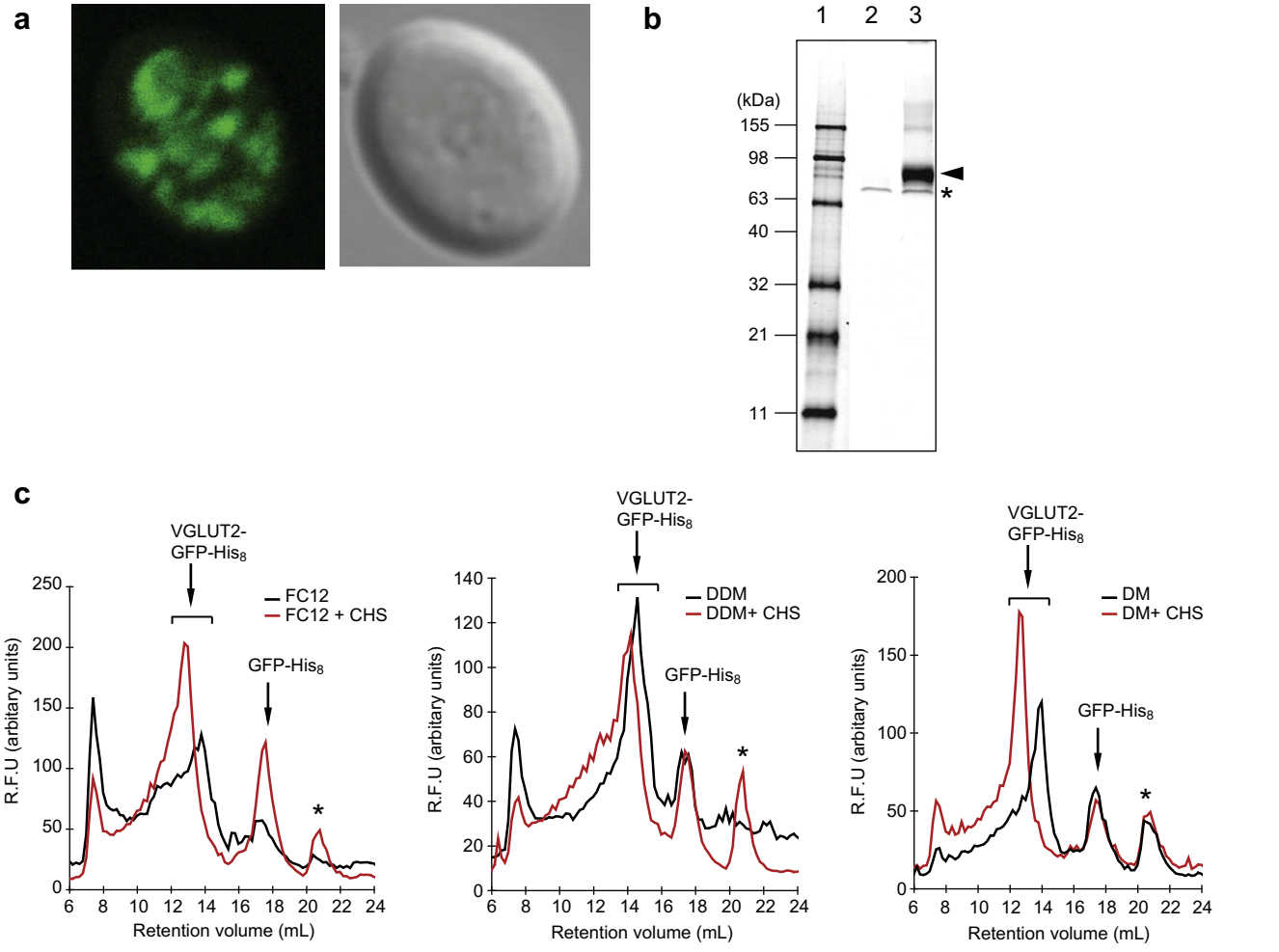

Fig. 4. Overexpression and monodispersity screening of rat VGLUT2–GFP–His_8 fusion in *S. cerevisiae*. (a) Typical confocal image of VGLUT2–GFP–His_8 localization in *S. cerevisiae* cells. Left and right panel indicate fluorescence and differential interference contrast images, respectively. (b) In-gel fluorescence detection of VGLUT2–GFP–His_8 expression. 1, fluorescent protein standard; 2, membranes isolated from cells harboring empty vector; 3, membranes from cells overexpressing VGLUT2–GFP–His_8; arrowhead and asterisk indicate VGLUT2–GFP–His_8 fusion and endogenous fluorescent background protein, respectively. (c) FSEC profiles of VGLUT2–GFP–His_8 in detergent-solubilized membrane in the presence (red) or absence (black) of 0.2% w/v CHS. *Note*: detergent-solubilized membranes were injected onto a Superose 6 10/300 column (GE-healthcare) and fractionated 0.2 ml into 96-well plate (Nunc™). Fluorescence was measured at 512 nm by excitation at 470 nm; asterisk indicates endogenous fluorescent protein.

however, there was a large 'free' GFP peak that suggests further VGLUT2 degradation during purification (Fig. 5a). Although the *S. cerevisiae* strain used for membrane protein overexpression has the *pep4* gene coding for the vacuolar protease deleted and protease inhibitors are used during purification, proteolysis for VGLUT2 is still a problem. For this reason we engineered an N-terminal FLAG tag on the basis of a study that showed degradation of the H^+-ATPase Pma1p in *S. cerevisiae* could be minimized by addition of a soluble N-terminal fusion [56].

The recovery of VGLUT2–GFP–His_8 after purification was improved in the presence of the FLAG tag, and was used in an additional tag for purification (Fig. 5a). After IMAC and FLAG tag purification, ~1 mg of pure VGLUT2–GFP–His_8 was isolated from 10 l of yeast culture (Fig. 5b). The transport of L-glutamate by VGLUT2 requires a membrane potential [48]. We incorporated the VGLUT2–GFP–His_8 fusion, VGLUT2 after GFP–His_8 removal, and VGLUT2–His_6 purified from insect cells together with bacterial F_0F_1-ATPase into proteoliposomes and measured ATP dependent L-glutamate uptake (Fig. 5c) [55]. Purified VGLUT2–GFP–His_8 and VGLUT2 from *S. cerevisiae* cells possesses almost identical functional activity to that of VGLUT2 purified from insect cells.

4.2. Case study 2: facilitative glucose transporter, GLUT1

Glucose is an essential energy source for mammalian cells. Mammalian glucose transporters are classified into two distinct groups, sodium glucose cotransporters (SGLT) and facilitative glucose transporters (GLUT). SGLT1 and SGLT2 transport glucose by a secondary-active transport mechanism [57], while several GLUTs mediate passive transport of glucose [58]. Among 14 GLUT members, GLUT1 is well characterized and is widely distributed into many tissues, especially abundant in human erythrocytes. Since the first identification of GLUT1 purified from Triton X-100-solubilized membranes [59], many research groups have isolated human GLUT1 from erythrocyte membranes by ion exchange chromatography [60–64]. However, it seems probable that heterogeneous glycosylation [65] has been an obstacle to crystallize GLUT1 purified from this native source [64].

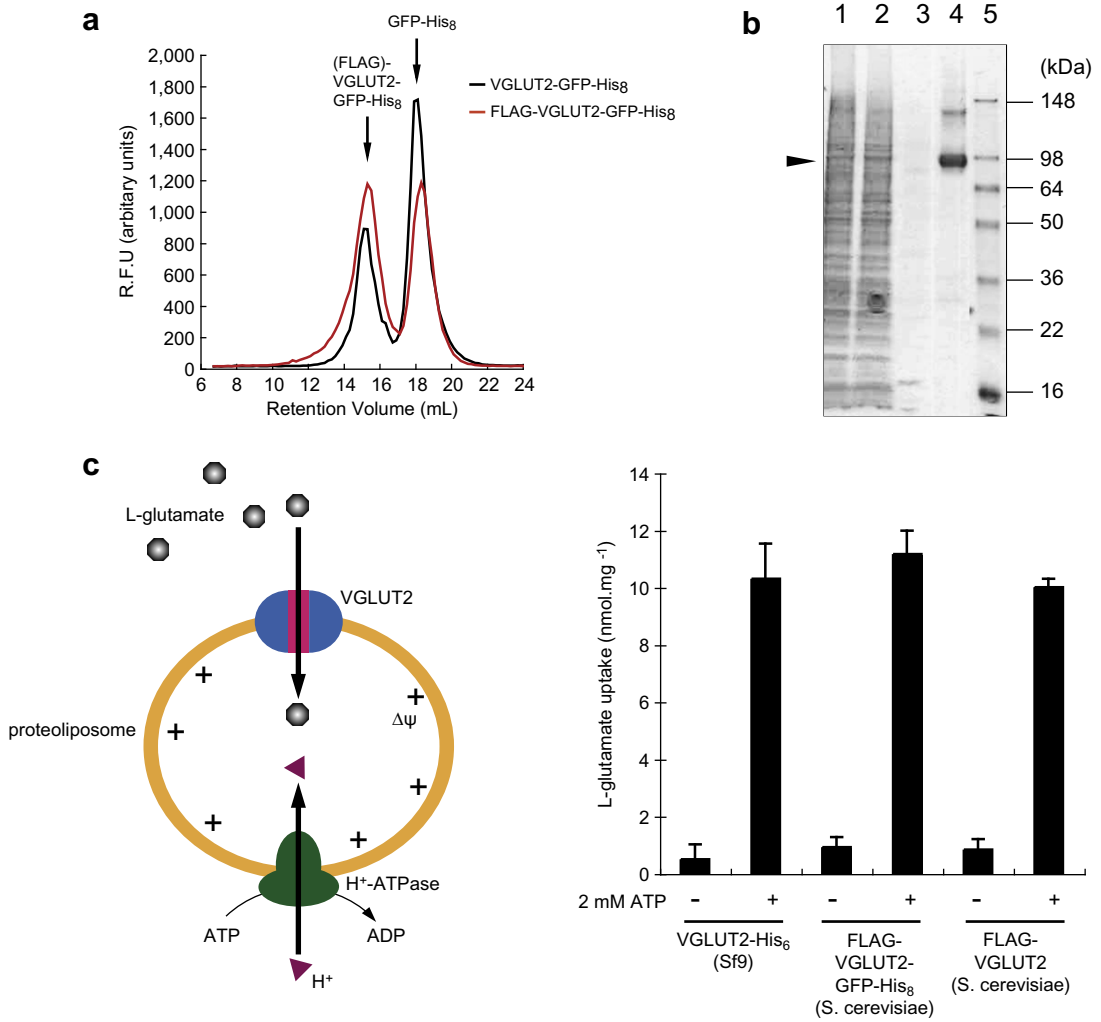

Fig. 5. Purification and functional assessment of purified rat VGLUT2 from *S. cerevisiae*. (a) FSEC profile of purified VGLUT2–GFP–His_8 fusion with (red) or without (black) N-terminal FLAG tag after Ni-NTA purification. GFP-fusion peak and 'free' GFP peak are indicated by arrow in the upper side of each peak. (b) Coomassie stained SDS-gel depicting purification of VGLUT2. 1, total membranes; 2, DM plus CHS-solubilized membranes; 3, Ni-NTA eluate after IMAC purification of membranes solubilized in 1% DM with 0.2% CHS; 4, FLAG eluate after FLAG tag purification of fraction shown in lane 3; and 5, pre-stained molecular weight (MW) protein ladder. (c) ATP dependent L-glutamate uptake by reconstituted VGLUT2. The illustration on left shows the transport mechanism of VGLUT2 in proteoliposomes. VGLUT2-His_6 protein was purified in OG from HighFive cells as described previously [55]; GFP-tag was removed from FLAG-VGLUT2–GFP–His_8 by His_6-tagged tobacco etch virus protease followed by removal of tag and GFP–His_8 by passing through a 5-ml His-Trap™ column (GE-healthcare) as described in detail in Ref. [9]. The detergent was exchanged into OG prior to reconstitution into proteoliposomes with the bacterial F_0F_1-ATPase. The ATP-dependent transport activity of each VGLUT2 fraction was assessed as previously described [55].

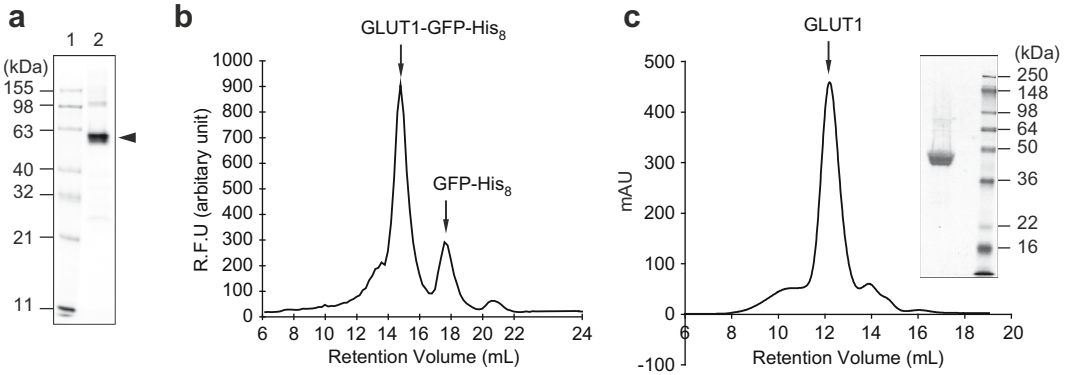

Fig. 6. Purification of human GLUT1 from *S. cerevisiae*. (a) In-gel fluorescence detection after SDS–PAGE. 1, fluorescent protein standard; 2, membranes from GLUT1–GFP–His_8 expressing yeast cells (b) FSEC profile of human GLUT1–GFP–His_8 in DDM-solubilized membranes (c) left, SEC profile of human GLUT1 and right, purified GLUT1 as judged by Coomassie staining after SDS–PAGE.

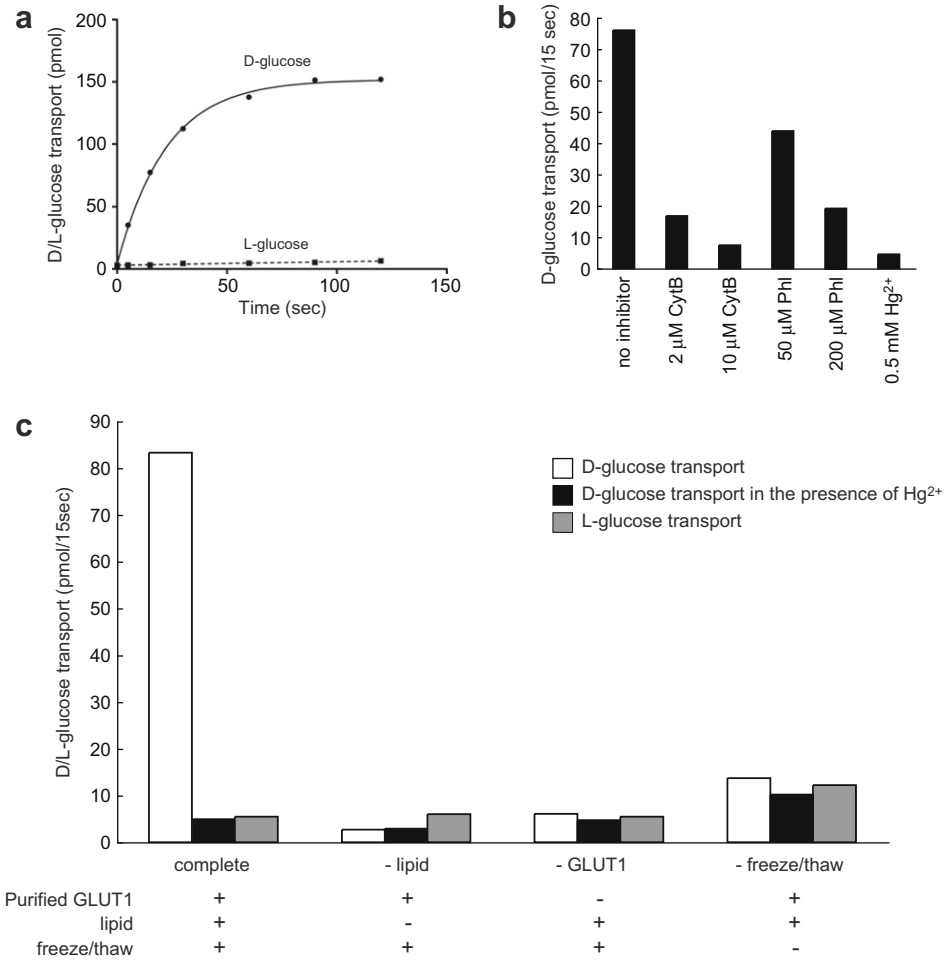

Fig. 7. Transport activity of reconstituted GLUT1. Purified GLUT1 was reconstituted by freeze–thaw/extrusion method. Briefly, crude lipid was extracted from bovine liver [71], and the lipid was sonicated to make unilamellar liposomes. 500 μL of a mixture containing ~10 μg of purified GLUT1 and 20 mg of liposomes in 10 mM $TrisSO_4$ (pH 7.5) was flash frozen and thawed at room temperature. Large, unilamellar proteoliposomes were prepared by extrusion 11 times (LiposoFast, Avestin; membrane pore size, 400 nm). D-Glucose transport activity was measured with 0.1 mM [^{14}C] D-glucose at 25 °C in transport buffer containing 10 mM $TrisSO_4$ and 2 mM $MgSO_4$ (pH 7.5) as described [69]. (a) Time course of D-glucose transport in proteoliposomes (0.1 μg GLUT1, 0.6 mg lipid) was measured (solid line). Non-specific uptake was estimated with 0.1 mM [^{14}C] L-glucose (dashed line). (b) Effect of specific inhibitor. D-Glucose transport activities were measured in duplicate for 15 s after incubation with indicated inhibitor for more than 5 min at 25 °C. Average values of a representative experiment out of three are shown. (c) Requirement of GLUT1, lipid and freeze–thaw treatment. Reconstitution was performed in the presence of GLUT1 and lipid with freeze–thaw treatment (complete), or in the absence of lipid (-lipid) or GLUT1 (-GLUT1), or without freeze–thaw treatment (-freeze–thaw). D-Glucose transport was measured for 15 s in the absence (white bar) or presence (black bar) of 0.5 mM $HgCl_2$. L-Glucose transport was similarly measured without the addition of $HgCl_2$ (gray bar).

Recently, it was reported that GLUT1 could be successfully overproduced and purified from *Pichia pastoris* [66] and *Schizosaccharomyces pombe* [67]. We have also been working with GLUT proteins, and the GLUT1–GFP–His_8 construct overexpresses in *S. cerevisiae* at

~2 mg per liter of culture (Fig. 6a). Monitoring by FSEC it is clear that GLUT1–GFP–His_8 migrates as a symmetrical monodisperse peak in DDM-solubilized membranes (Fig. 6b). Our standard purification protocol after IMAC is to cleave the purified GFP–His_8 fusion with equimolar His_6-TEV protease during dialysis overnight at 10 °C. The reason for this is twofold, first dialysis dilutes out imidazole and secondly we equilibrate into the buffer used for crystallization. Dialysis into the crystallization buffer adds the extra option to use this material directly for crystallization, as there remains the possibility that omitting SEC produces better crystals [68]. Passing the digested material through a 5-ml HisTrap™ column in the absence of imidazole, the cleaved GFP–His_8 fusion, His_6-TEV protease and remaining inadvertent contaminants bind to the resin. By collecting the flow-through from the HisTrap™ column pure GLUT1 was recovered (Fig. 6c). The final yield of GLUT1 is 2 mg from 10 l of yeast culture.

GLUT1 was reconstituted into liposomes by a freeze–thaw/extrusion method. D-Glucose transport and non-specific L-glucose uptake into GLUT1 proteoliposomes was measured as described previously (Fig. 7a) [69]. As expected, the known inhibitors cytochalasin B and phloretin significantly inhibited D-glucose transport (Fig. 7b). Interestingly, after mixing purified GLUT1 with lipids, successful reconstitution was found to be best by including a freeze/thaw treatment (Fig. 7c); as far as we are aware this is the first time the importance of this step has been noted. Using this similar strategy we have been able to purify milligram amounts of several mammalian GLUTs in an active form (unpublished data).

Acknowledgements

We gratefully thank Narinobu Juge for work with VGLUT2 and Jan-Willem de Gier for critical reading of the manuscript. We wish to thank the Membrane Protein Laboratory (MPL) at the Diamond Light Source Limited for use of the MPL facilities. This research was funded primarily by the UK Biotechnology and Biological Sciences Research Council (Grant No. BB/C515163/1 to S.I.) with important contributions from the Membrane Protein Structure Initiative (Grant No. BBS/B/14418 to S.I.), and in part by the Royal Society (United Kingdom) through a University Research Fellowship (to D.D.).

References

[1] Deisenhofer, J., Epp, O., Miki, K., Huber, R. and Michel, H. (1985) Structure of the protein subunits in the photosynthetic reaction centre of *Rhodopseudomonas viridis* at 3 Å resolution. Nature 318, 618–624.
[2] Overington, J.P., Al-Lazikani, B. and Hopkins, A.L. (2006) How many drug targets are there? Nat. Rev. Drug Discov. 5, 993–996.
[3] Waldo, G.S., Standish, B.M., Berendzen, J. and Terwilliger, T.C. (1999) Rapid protein-folding assay using green fluorescent protein. Nat. Biotechnol. 17, 691–695.
[4] Luirink, J., von Heijne, G., Houben, E. and de Gier, J.W. (2005) Biogenesis of inner membrane proteins in *Escherichia coli*. Annu. Rev. Microbiol. 59, 329–355.
[5] Chang, H.C., Kaiser, C.M., Hartl, F.U. and Barral, J.M. (2005) De novo folding of GFP fusion proteins: high efficiency in eukaryotes but not in bacteria. J. Mol. Biol. 353, 397–409.
[6] Drew, D.E., von Heijne, G., Nordlund, P. and de Gier, J.W. (2001) Green fluorescent protein as an indicator to monitor membrane protein overexpression in *Escherichia coli*. FEBS Lett. 507, 220–224.
[7] Drew, D., Lerch, M., Kunji, E., Slotboom, D.J. and de Gier, J.W. (2006) Optimization of membrane protein overexpression and purification using GFP fusions. Nat. Meth. 3, 303–313.
[8] Drew, D., Slotboom, D.J., Friso, G., Reda, T., Genevaux, P., Rapp, M., Meindl-Beinker, N.M., Lambert, W., Lerch, M., Daley, D.O., Van Wijk, K.J., Hirst, J., Kunji, E. and De Gier, J.W. (2005) A scalable, GFP-based pipeline for membrane protein overexpression screening and purification. Protein Sci. 14, 2011–2017.
[9] Drew, D., Newstead, S., Sonoda, Y., Kim, H., von Heijne, G. and Iwata, S. (2008) GFP-based optimization scheme for the overexpression and purification of eukaryotic membrane proteins in *Saccharomyces cerevisiae*. Nat. Protoc. 3, 784–798.
[10] Newstead, S., Kim, H., von Heijne, G., Iwata, S. and Drew, D. (2007) High-throughput fluorescent-based optimization of eukaryotic membrane protein overexpression and purification in *Saccharomyces cerevisiae*. Proc. Natl. Acad. Sci. USA 104, 13936–13941.
[11] Kawate, T. and Gouaux, E. (2006) Fluorescence-detection size-exclusion chromatography for precrystallization screening of integral membrane proteins. Structure 14, 673–681.
[12] Wagner, S., Bader, M.L., Drew, D. and de Gier, J.W. (2006) Rationalizing membrane protein overexpression. Trends Biotechnol. 24, 364–371.
[13] Tate, C.G. (2001) Overexpression of mammalian integral membrane proteins for structural studies. FEBS Lett. 504, 94–98.
[14] Freigassner, M., Pichler, H. and Glieder, A. (2009) Tuning microbial hosts for membrane protein production. Microb. Cell Fact. 8, 69.
[15] Sobolevsky, A.I., Rosconi, M.P. and Gouaux, E. (2009) X-ray structure, symmetry and mechanism of an AMPA-subtype glutamate receptor. Nature 462, 745–756.
[16] Tate, C.G., Haase, J., Baker, C., Boorsma, M., Magnani, F., Vallis, Y. and Williams, D.C. (2003) Comparison of seven different heterologous protein expression systems for the production of the serotonin transporter. Biochim. Biophys. Acta 1610, 141–153.
[17] Newstead, S., Ferrandon, S. and Iwata, S. (2008) Rationalizing alpha-helical membrane protein crystallization. Protein Sci. 17, 466–472.
[18] Fucile, S., Palma, E., Martinez-Torres, A., Miledi, R. and Eusebi, F. (2002) The single-channel properties of human acetylcholine alpha 7 receptors are altered by fusing alpha 7 to the green fluorescent protein. Proc. Natl. Acad. Sci. USA 99, 3956–3961.
[19] Huh, W.K., Falvo, J.V., Gerke, L.C., Carroll, A.S., Howson, R.W., Weissman, J.S. and O'Shea, E.K. (2003) Global analysis of protein localization in budding yeast. Nature 425, 686–691.
[20] Sato, K., Sato, M. and Nakano, A. (2001) Rer1p, a retrieval receptor for endoplasmic reticulum membrane proteins, is dynamically localized to the Golgi apparatus by coatomer. J. Cell Biol. 152, 935–944.
[21] Drew, D., Sjostrand, D., Nilsson, J., Urbig, T., Chin, C.N., de Gier, J.W. and von Heijne, G. (2002) Rapid topology mapping of *Escherichia coli* inner-membrane proteins by prediction and PhoA/GFP fusion analysis. Proc. Natl. Acad. Sci. USA 99, 2690–2695.
[22] Daley, D.O., Rapp, M., Granseth, E., Melen, K., Drew, D. and von Heijne, G. (2005) Global topology analysis of the *Escherichia coli* inner membrane proteome. Science 308, 1321–1323.
[23] Quick, M. and Wright, E.M. (2002) Employing *Escherichia coli* to functionally express, purify, and characterize a human transporter. Proc. Natl. Acad. Sci. USA 99, 8597–8601.
[24] Hsieh, J.M., Besserer, G.M., Madej, M.G., Bui, H.Q., Kwon, S. and Abramson, J. (2010) Bridging the gap: a GFP-based strategy for overexpression and purification of membrane proteins with intra and extracellular C-termini. Protein Sci. 19, 868–880.
[25] Yano, Y. and Matsuzaki, K. (2009) Tag-probe labeling methods for live-cell imaging of membrane proteins. Biochim. Biophys. Acta 1788, 2124–2131.
[26] Michel, H. (2001) Crystallization of membrane proteins in: International Tables for Crystallograpy (Rossman, M. and Arnold, E., Eds.), pp. 94–100, Kluwer Academic Publishers, Dordercht.
[27] Faham, S., Watanabe, A., Besserer, G.M., Cascio, D., Specht, A., Hirayama, B.A., Wright, E.M. and Abramson, J. (2008) The crystal structure of a sodium galactose transporter reveals mechanistic insights into Na^+/sugar symport. Science 321, 810–814.
[28] Weyand, S., Shimamura, T., Yajima, S., Suzuki, S., Mirza, O., Krusong, K., Carpenter, E.P., Rutherford, N.G., Hadden, J.M., O'Reilly, J., Ma, P., Saidijam, M., Patching, S.G., Hope, R.J., Norbertczak, H.T., Roach, P.C., Iwata, S., Henderson, P.J. and Cameron, A.D. (2008) Structure and molecular mechanism of a nucleobase-cation-symport-1 family transporter. Science 322, 709–713.
[29] Yamashita, A., Singh, S.K., Kawate, T., Jin, Y. and Gouaux, E. (2005) Crystal structure of a bacterial homologue of Na^+/Cl-dependent neurotransmitter transporters. Nature 437, 215–223.
[30] Shaffer, P.L., Goehring, A., Shankaranarayanan, A. and Gouaux, E. (2009) Structure and mechanism of a Na^+-independent amino acid transporter. Science 325, 1010–1014.
[31] Iwata, S., Ostermeier, C., Ludwig, B. and Michel, H. (1995) Structure at 2.8 Å resolution of cytochrome *c* oxidase from *Paracoccus denitrificans*. Nature 376, 660–669.
[32] Jiang, Y., Lee, A., Chen, J., Ruta, V., Cadene, M., Chait, B.T. and MacKinnon, R. (2003) X-ray structure of a voltage-dependent K^+ channel. Nature 423, 33–41.
[33] Rasmussen, S.G., Choi, H.J., Rosenbaum, D.M., Kobilka, T.S., Thian, F.S., Edwards, P.C., Burghammer, M., Ratnala, V.R., Sanishvili, R., Fischetti, R.F., Schertler, G.F., Weis, W.I. and Kobilka, B.K. (2007) Crystal structure of the human beta2 adrenergic G-protein-coupled receptor. Nature 450, 383–387.
[34] Dutzler, R., Campbell, E.B., Cadene, M., Chait, B.T. and MacKinnon, R. (2002) X-ray structure of a ClC chloride channel at 3.0 Å reveals the molecular basis of anion selectivity. Nature 415, 287–294.
[35] Dutzler, R., Campbell, E.B. and MacKinnon, R. (2003) Gating the selectivity filter in ClC chloride channels. Science 300, 108–112.
[36] Sennhauser, G. and Grutter, M.G. (2008) Chaperone-assisted crystallography with DARPins. Structure 16, 1443–1453.
[37] Sennhauser, G., Amstutz, P., Briand, C., Storchenegger, O. and Grutter, M.G. (2007) Drug export pathway of multidrug exporter AcrB revealed by DARPin inhibitors. PLoS Biol. 5, e7.
[38] Cherezov, V., Rosenbaum, D.M., Hanson, M.A., Rasmussen, S.G., Thian, F.S., Kobilka, T.S., Choi, H.J., Kuhn, P., Weis, W.I., Kobilka, B.K. and Stevens, R.C.

(2007) High-resolution crystal structure of an engineered human beta2-adrenergic G protein-coupled receptor. Science 318, 1258–1265.
[39] Hanson, M.A. and Stevens, R.C. (2009) Discovery of new GPCR biology: one receptor structure at a time. Structure 17, 8–14.
[40] Bowie, J.U. (2001) Stabilizing membrane proteins. Curr. Opin. Struct. Biol. 11, 397–402.
[41] Lau, F.W. and Bowie, J.U. (1997) A method for assessing the stability of a membrane protein. Biochemistry 36, 5884–5892.
[42] Warne, T., Serrano-Vega, M.J., Baker, J.G., Moukhametzianov, R., Edwards, P.C., Henderson, R., Leslie, A.G., Tate, C.G. and Schertler, G.F. (2008) Structure of a beta1-adrenergic G-protein-coupled receptor. Nature 454, 486–491.
[43] Serrano-Vega, M.J., Magnani, F., Shibata, Y. and Tate, C.G. (2008) Conformational thermostabilization of the beta1-adrenergic receptor in a detergent-resistant form. Proc. Natl. Acad. Sci. USA 105, 877–882.
[44] Alexandrov, A.I., Mileni, M., Chien, E.Y., Hanson, M.A. and Stevens, R.C. (2008) Microscale fluorescent thermal stability assay for membrane proteins. Structure 16, 351–359.
[45] Hanson, M.A., Cherezov, V., Griffith, M.T., Roth, C.B., Jaakola, V.P., Chien, E.Y., Velasquez, J., Kuhn, P. and Stevens, R.C. (2008) A specific cholesterol binding site is established by the 2.8 Å structure of the human beta2-adrenergic receptor. Structure 16, 897–905.
[46] Abramson, J., Smirnova, I., Kasho, V., Verner, G., Kaback, H.R. and Iwata, S. (2003) Structure and mechanism of the lactose permease of *Escherichia coli*. Science 301, 610–615.
[47] Chaptal, V., Ujwal, R., Nie, Y., Watanabe, A., Kwon, S. and Abramson, J. (in press) Fluorescence Detection of Heavy Atom Labeling (FD-HAL): a rapid method for identifying covalently modified cysteine residues by phasing atoms. J. Struct. Biol.
[48] Fremeau Jr., R.T., Voglmaier, S., Seal, R.P. and Edwards, R.H. (2004) VGLUTs define subsets of excitatory neurons and suggest novel roles for glutamate. Trends Neurosci. 27, 98–103.
[49] Moriyama, Y. and Yamamoto, A. (2004) Glutamatergic chemical transmission: look! Here, there, and anywhere. J. Biochem. 135, 155–163.
[50] Edwards, R.H. (2007) The neurotransmitter cycle and quantal size. Neuron 55, 835–858.
[51] Maycox, P.R., Hell, J.W. and Jahn, R. (1990) Amino acid neurotransmission: spotlight on synaptic vesicles. Trends Neurosci. 13, 83–87.
[52] Hayashi, M., Otsuka, M., Morimoto, R., Hirota, S., Yatsushiro, S., Takeda, J., Yamamoto, A. and Moriyama, Y. (2001) Differentiation-associated Na^+-dependent inorganic phosphate cotransporter (DNPI) is a vesicular glutamate transporter in endocrine glutamatergic systems. J. Biol. Chem. 276, 43400–43406.
[53] Burger, K., Gimpl, G. and Fahrenholz, F. (2000) Regulation of receptor function by cholesterol. Cell Mol. Life Sci. 57, 1577–1592.
[54] van der Rest, M.E., Kamminga, A.H., Nakano, A., Anraku, Y., Poolman, B. and Konings, W.N. (1995) The plasma membrane of *Saccharomyces cerevisiae*: structure, function, and biogenesis. Microbiol. Rev. 59, 304–322.
[55] Juge, N., Yoshida, Y., Yatsushiro, S., Omote, H. and Moriyama, Y. (2006) Vesicular glutamate transporter contains two independent transport machineries. J. Biol. Chem. 281, 39499–39506.
[56] Liu, Y., Sitaraman, S. and Chang, A. (2006) Multiple degradation pathways for misfolded mutants of the yeast plasma membrane ATPase, Pma1. J. Biol. Chem. 281, 31457–31466.
[57] Wright, E.M. and Turk, E. (2004) The sodium/glucose cotransport family SLC5. Pflugers Arch. 447, 510–518.
[58] Uldry, M. and Thorens, B. (2004) The SLC2 family of facilitated hexose and polyol transporters. Pflugers Arch. 447, 480–489.
[59] Kasahara, M. and Hinkle, P.C. (1977) Reconstitution and purification of the D-glucose transporter from human erythrocytes. J. Biol. Chem. 252, 7384–7390.
[60] Cairns, M.T., Elliot, D.A., Scudder, P.R. and Baldwin, S.A. (1984) Proteolytic and chemical dissection of the human erythrocyte glucose transporter. Biochem. J. 221, 179–188.
[61] Hebert, D.N. and Carruthers, A. (1991) Cholate-solubilized erythrocyte glucose transporters exist as a mixture of homodimers and homotetramers. Biochemistry 30, 4654–4658.
[62] Lundahl, P., Greijer, E., Cardell, S., Mascher, E. and Andersson, L. (1986) Improved preparation of the integral membrane proteins of human red cells, with special reference to the glucose transporter. Biochim. Biophys. Acta 855, 345–356.
[63] Rampal, A.L., Jung, E.K., Chin, J.J., Deziel, M.R., Pinkofsky, H.B. and Jung, C.Y. (1986) Further characterization and chemical purity assessment of the human erythrocyte glucose transporter preparation. Biochim. Biophys. Acta 859, 135–142.
[64] Boulter, J.M. and Wang, D.N. (2001) Purification and characterization of human erythrocyte glucose transporter in decylmaltoside detergent solution. Protein Expr. Purif. 22, 337–348.
[65] Endo, T., Kasahara, M. and Kobata, A. (1990) Structures of the asparagine-linked sugar chain of glucose transporter from human erythrocytes. Biochemistry 29, 9126–9134.
[66] Alisio, A. and Mueckler, M. (2010) Purification and characterization of mammalian glucose transporters expressed in *Pichia pastoris*. Protein Expr. Purif. 70, 81–87.
[67] Yang, Y., Hu, Z., Liu, Z., Wang, Y., Chen, X. and Chen, G. (2009) High human GLUT1, GLUT2, and GLUT3 expression in *Schizosaccharomyces pombe*. Biochemistry 74, 75–80.
[68] Guan, L., Mirza, O., Verner, G., Iwata, S. and Kaback, H.R. (2007) Structural determination of wild-type lactose permease. Proc. Natl. Acad. Sci. USA 104, 15294–15298.
[69] Kasahara, T. and Kasahara, M. (1996) Expression of the rat GLUT1 glucose transporter in the yeast *Saccharomyces cerevisiae*. Biochem. J. 315, 177–182.
[70] Roth, C.B., Hanson, M.A. and Stevens, R.C. (2008) Stabilization of the human beta2-adrenergic receptor TM4–TM3–TM5 helix interface by mutagenesis of Glu122(3.41), a critical residue in GPCR structure. J. Mol. Biol. 376, 1305–1319.
[71] Bligh, E.G. and Dyer, W.J. (1959) A rapid method of total lipid extraction and purification. Can. J. Biochem. Physiol. 37, 911–917.